Inorganic Chemistry

pubs.acs.org/IC Article

A Discrete Tetrahedral Indium Cage as an Efficient Heterogeneous Catalyst for the Fixation of CO_2 and the Strecker Reaction of Ketones

Guang-Ming Liang,[§] Peng Xiong,[§] Khan Azam, Qing-Ling Ni, Jian-Qiang Zeng,* Liu-Cheng Gui,* and Xiu-Jian Wang*

Cite This: https://dx.doi.org/10.1021/acs.inorgchem.9b02763 Read Online

ACCESS | Metrics & More | Article Recommendations | Supporting Information

ABSTRACT: A discrete tetrahedral indium cage, $\{[In_{12}(\mu_3\text{-}OH)_4(HCO_2)_{24}(tcma)_4]\}$ (In_{12}-GL), was synthesized solvothermally by the reaction of indium nitrate with the tripodal tricarboxylic acid ligand *N,N,N*-tris{(2′-carboxy[1,1′-biphenyl]-4-yl)methyl}methylammonium chloride ($[H_3tcma]^+Cl$). This cage consists of four trimeric units $[In_3(\mu_3\text{-}OH)(\mu_2\text{-}CO_2)_3(\mu_2\text{-}HCO_2)_3]$ and four $[tcma]^{2-}$ ligands, which all perform as 3-connection nodes to bridge each other, resulting in a tetrahedral cage structure. The trimeric unit $[In_3(\mu_3\text{-}OH)(\mu_2\text{-}CO_2)_3(\mu_2\text{-}HCO_2)_3]$ is observed for the first time in the family of In-based metal−organic structures and can be considered as an evolution of a 6-connected $[In_3(\mu_3\text{-}O)(\mu_2\text{-}CO_2)_6]$ unit. Each In^{3+} is terminally coordinated by a μ_1-HCO_2 group. This cage contains potential Lewis acidic/basic active sites endowed by In^{3+} ions as Lewis acidic sites and the uncoordinated oxygen atoms of μ_1-HCO_2 moieties as Lewis basic sites and was explored as an effective heterogeneous catalyst in the cycloaddition of CO_2 with epoxides and the Strecker reaction for amino nitriles. These catalytic reactions were deduced to happen on the surface of the In_{12}-GL cage.

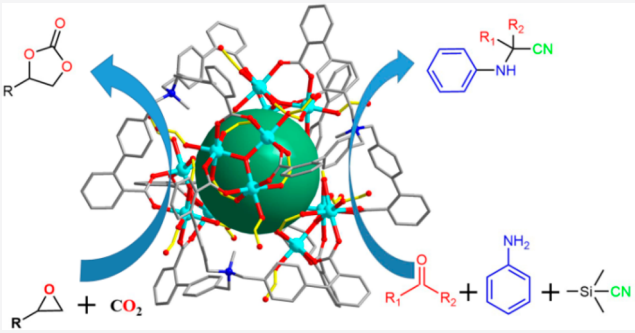

INTRODUCTION

Metal−organic porous materials (MOPMs), including metal−organic frameworks (MOFs) and discrete metal−organic cages (MOCs) constructed from inorganic metal ions or clusters with bridging organic ligands, have been reported recently as interesting and promising heterogeneous catalysts, due to their highly specific porous features, large surface areas, and multiple catalytic sites.[1−21] The transition metals in MOPM can be endowed with catalytically active sites for a wide variety of organic reactions. These porous structures allow the substrates to diffuse through the pores/channels to react with the catalytically active sites located within the cavity.[22−27] The Lewis base active sites can also be introduced at different locations of the metal−organic porous structure for synergistic catalysis.[28−30] The high content of these active sites in MOPMs is advantageous for catalytic reactions.

However, the low thermal, chemical, and solvent stability of MOPMs restricts their applications in catalytic organic reactions. The commonly feasible solution is to exploit polydentate and/or rigid organic ligands to construct stable MOPMs.[31−37] In addition, various strategies for boosting MOF stability have been explored by enhancing the interactions of metal−ligand bonds and/or shielding inorganic ions/clusters from unfeasible environments. A potential instability has been generated commonly in MOPMs during the effective activation process of open Lewis acid sites by removal of solvents and media within the pores/channels before the catalytic reaction. Relatively, the pretreatment of stable MOCs is much simpler and easier than for 3D MOFs, since the active metal sites are usually located on the surface of MOCs, to which the accessibility of reactive substrates is very easy and feasible. The solvents within the pores of MOCs have little influence on the catalytic reactions taking place at the cage surface.

The main-group-metal ions, especially those with large radii such as Sr^{2+}, Ba^{2+}, Ga^{3+}, and In^{3+}, have versatile coordination numbers, which makes them excellent candidates as Lewis acid catalysts. The In^{3+} cation is liable to form thermally and chemically stable MOFs, due to its high charge density possibly inducing strong coordination with organic ligands.[38−48] These MOFs have been proven to be promising candidates in gas storage/separation, Lewis acid chemical catalysis, and photocatalysis in organic transformations. Among some of these MOFs, the interesting indium-containing trimeric unit $[In_3(\mu_3\text{-}O)(O_2C)_6]$ performs as a secondary building unit for 6-connected 3D networks.[43,44] As we know that there has been

Received: September 18, 2019

Scheme 1. Schematic Diagram of Ligand $[H_3tcma]^+Cl$ and Synthetic Scheme of In_{12}-GL[a]

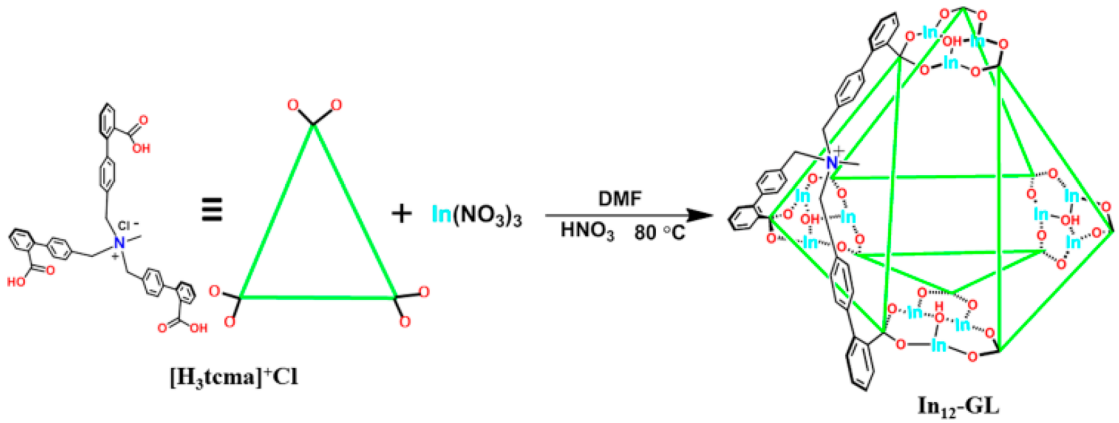

[a]HCO_2^- groups are deleted for clarity.

no In-based discrete MOC reported until now, therefore, construction of novel indium-based structures can not only enrich the structural features but also enable fine functionalization. In this paper, we synthesized a new tripodal tricarboxylate ligand, *N,N,N*-tris{(2′-carboxy[1,1′-biphenyl]-4-yl)methyl}-methylammonium chloride ($[H_3tcma]^+Cl$), which has structural features of semirigidity, a charge-separated skeleton, a degree of spatial confinement, and coordination direction. The reaction of $[H_3tcma^+]Cl$ with $In(NO_3)_3$ in DMF in the presence of nitric acid afforded white octahedral crystals of the complex $\{[In_{12}(\mu_3\text{-}OH)_4(HCO_2)_{24}(tcma)_4]\}$ (In_{12}-GL) (Scheme 1).

■ EXPERIMENTAL SECTION

Materials and Methods. All chemicals and solvents were purchased from available commercial sources and used as received. IR spectra were recorded as KBr pellets on a PerkinElmer FT-IR spectrometer in the range 4000−450 cm^{-1}. Thermogravimetric analysis (TGA) was measured on a Labsys evo TG-DTA/DSC thermal analyzer under a nitrogen atmosphere with a heating rate of 5 °C/min. Powder X-ray diffraction (PXRD) data were collected on a Rigaku D/Max 2500 diffractometer (Cu Kα, λ = 1.5418 Å) and 2θ ranging from 5 to 50°. The yield of isolated product was determined by GC-MS equipment (Agilent 5977B). ^{1}H NMR spectra were recorded on an AVANCE 3HD (400 MHz) instrument in DMSO-d_6 with Me_4Si as the internal standard. ESI-MS mass spectra were recorded on a Bruker HCT mass spectrometer. Scanning electron microscopy (SEM) and elemental mapping spectra were carried out on a FEI Quanta 200 instrument (Oxford Instruments). Gas adsorption−desorption measurements were acquired on a PS2-1001 surface area analyzer with a desorption temperature of 100 °C under vacuum.

Synthesis of the Ligand $[H_3tcma]^+Cl$. A 30% solution of $MeNH_2$ in ethanol (1 mL, ρ = 0.66 g mL^{-1}, containing 6.38 mmol of $MeNH_2$) was added to a solution of 20 mL of dry CH_3CH_2OH containing 4′-(bromomethyl)biphenyl-2-carboxylic acid methyl ester (5.84 g, 19.14 mmol). After the solution mixture was refluxed at 80 °C for 8 h with stirring, 10% NaOH aqueous solution (~25 mL) was added and the solution mixture was further refluxed for another 8 h. Then the reaction solution was cooled to room temperature. A hydrochloric acid solution (1 mol L^{-1}) was added dropwise into the reaction solution, adjusting the pH to 7, at which point white precipitates appeared. The resulting white precipitates were washed using CH_2Cl_2 and then recrystallized in CH_3OH solution to produce white crystals. Yield: 2.67 g (60%). ESI-MS: 662.25 for $[H_3tcma]^+$. ^{1}H NMR: δ 2.94 (3H), 4.58 (6H), 7.39 (3H), 7.45 (9H), 7.58 (9H),7.70 (3H). IR (cm^{-1}): 3460(br), 1704(vs), 1470(s), 1372(s), 1256(s), 1220(s), 1003(m), 912(s), 847(s), 759(s), 534(s), 416(w).

Synthesis of $\{[In_{12}(\mu_3\text{-}OH)_4(HCO_2)_{24}(tcma)_4]\cdot x(solvent)\}$ ($[In_{12}\text{-}GL]\cdot x(solvent)$). A mixture of $[H_3tcma]^+Cl$ (0.06624 g, 0.1 mmol) and $In(NO_3)_3\cdot xH_2O$ (0.12 g, 0.4 mmol) was dissolved in DMF (12 mL) in a Teflon-lined stainless steel autoclave, and then concentrated nitric acid (0.1 mL) was added. The autoclave was heated at 80 °C under autogenous pressure for 7 days, followed by cooling to room temperature. Pure white octahedral crystals were obtained after centrifugation and washing with DMF. Powder X-ray diffraction of the as-synthesized sample shows it is a pure phase. Yield: 0.15 g, 60% based on In^{3+} ion. IR (cm^{-1}): 3432 (br), 1600 (vs), 1473 (m), 1386 (s), 1307 (m), 853 (s), 764 (s), 628 (s), 533 (w), 458 (m).

X-ray Structural Studies. The X-ray single-crystal diffraction data of In_{12}-GL were recorded on the BL17B beamline (λ = 0.72 Å) at the Shanghai Synchrotron Radiation Facility (SSRF) at 107 K. All calculations were performed with Olex2 and SHELXL crystallographic software packages. The structure was solved by standard direct methods and refined by anisotropic approximation. The solvent molecules were highly disordered. The diffused electron densities resulting from these residual solvent molecules were removed from the data set by using the SQUEEZE routine of PLATON. The solvent molecules were calculated on the basis of a combined study of TGA and the removed electron counts. The solvents are excluded from the unit cell contents in the crystal data. The crystal data and experimental details for In_{12}-GL are given in Table 1, and the selected bond distances and angles are shown in Table S1.

■ RESULTS AND DISCUSSION

Single-crystal X-ray diffraction analysis indicates that this compound crystallizes in the cubic $Fd\bar{3}$ space group and has a tetrahedral cage structure. Its asymmetric unit contains one-third of the ligand, one μ_3-OH^- anion, one In^{3+} ion, and two formate groups (Figure 1). This tetrahedral cage consists of the trimeric anionic unit $[In_3(OH)(\mu_2\text{-}CO_2)_3(\mu_2\text{-}HCO_2)_3]$ formed by three indium atoms sharing a central hydroxyl anion, bridged respectively by three formates and three carboxylate groups from the $[tcma]^{2-}$ linkers (Figure 2). Each In^{3+} ion is terminated by a formate anion. These formate anions are likely produced by the decomposition of DMF during the In_{12}-GL formation reaction. The trimeric $[In_3(\mu_3\text{-}OH)(\mu_2\text{-}CO_2)_3(\mu_2\text{-}HCO_2)_3]$ unit can be thought as an evolution from the 6-connected $[In_3(\mu_3\text{-}O)(\mu_2\text{-}CO_2)_6]$ unit, of which three μ_2-CO_2 moieties are replaced by three μ_2-HCO_2 groups and the central μ_3-O is replaced by μ_3-OH. This indium-containing unit $[In_3(\mu_3\text{-}OH)(\mu_2\text{-}CO_2)_3(\mu_2\text{-}HCO_2)_3]$ performs as a 3-connected unit which has been observed for the first time in In-based complexes. Meanwhile the geometric configuration of the ligand $[tcma]^{2-}$ matches with this 3-connected trimeric

https://dx.doi.org/10.1021/acs.inorgchem.9b02763
Inorg. Chem. XXXX, XXX, XXX−XXX

Table 1. Crystal Data and Structure Refinement Details for In_{12}-GL

empirical formula	$C_{196}H_{160}In_{12}N_4O_{76}$
formula wt	5165.11
crystal system	cubic
space group	$Fd\bar{3}$
a (Å)	45.883(5)
b (Å)	45.883(5)
c (Å)	45.883(5)
α (deg)	90
β (deg)	90
γ (deg)	90
V (Å^3)	96595(32)
Z	8
radiation	Synchrotron Radiation Facility (λ = 0.72 Å)
temp (K)	107
ρ_{calc} (g/cm^{-3})	0.710
μ (mm^{-1})	0.618
θ range for data collection (deg)	1.491−24.131
no. of rflns collected	68273
no. of indep rflns	5429
no. of data/restraints/params	6202/0/219
goodness of fit (GOF)	1.076
final R index ($I > 2\sigma(I)$)	0.0497
R index (all data)	0.0535
largest diff peak/hole (e Å^{-3})	0.323/−0.830

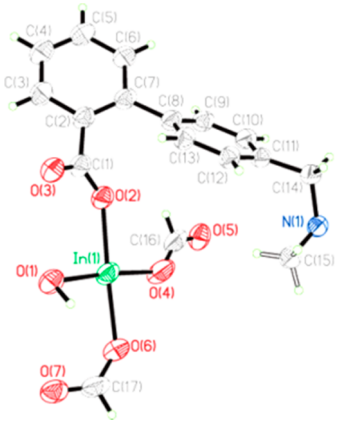

Figure 1. Asymmetric unit of In_{12}-GL with an ellipsoidal mode.

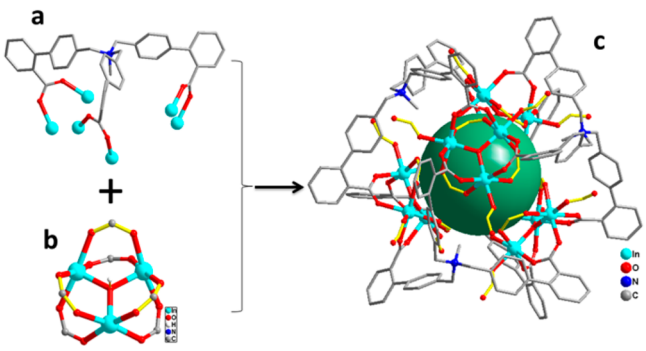

Figure 2. (a) Ligand coordination mode, (b) the trimeric unit of $[In_3(OH)(\mu_2\text{-}CO_2)_3(\mu_2\text{-}HCO_2)_3]$, and (c) the tetrahedral cage of In_{12}-GL. Bond colors: yellow, formate groups; gray, the carboxylate groups from ligands. H atoms are deleted for clarity.

unit, inducing the establishment of a tetrahedral cage in which four trimeric units are bridged mutually by four ligands. Nevertheless, the 6-connected indium based unit $[In_3(\mu_3\text{-}O)(\mu_2\text{-}CO_2)_6]$ is normally observed in 3-D porous structures.[33,46−48] For known In^{3+} carboxylate coordination frameworks, two other types of indium-based secondary building units are also very common in the documented In-MOF structures, including tetrahedral $[In(O_2CR)_4]$[9,27,43] and linear $[In(\mu\text{-}OH)(O_2CR)_2]$.[39,41,54] As we know, there have been only two discrete In^{3+} carboxylate polyhedra reported which were constructed on the basis of the flexible ligand 1,3,5-tris(4-carboxyphenoxy)benzene.[40]

Each In^{3+} ion in an octahedral coordination environment of InO_6 (Figure S3) consists of two oxygen atoms from different $[tcma]^{2-}$ ligands, two oxygen atoms from different μ_2-HCO_2 groups, one oxygen from OH^-, and one oxygen from a terminal μ_1-HCO_2. The ligand's cationic skeleton of this cage should be positive against the formation of the anionic moiety $[In_3(\mu_3\text{-}OH)(\mu_2\text{-}CO_2)_2(\mu_2\text{-}HCO_2)_3(\mu_1\text{-}HCO_2)_3]$ (Figure S4). The bridging formates extend toward the cage interior, while the terminal formates and tcma moieties extend outward, resulting in the formation of an indium cage with an aperture diameter of ∼8 Å and a small-sized window of ∼3.2 Å (Figure S5). All In^{3+} ions are exposed on the surface of In_{12}-GL and are easily accessible to the reactive substrates. This gives extra advantage by increasing the cage potential Lewis acid active sites and needs no special activation process for the catalytic reaction happening on the cage surfaces. Furthermore, the uncoordinated oxygen atom in the terminal μ_1-formate can act as a potential Lewis basic site for synergistic catalysis. Therefore, In_{12}-GL can have potential synergetic catalysis, and the catalytic reaction would take place on the surface due to the small window size. However, in most of the 3-D porous frameworks constructed by the trimeric $[In_3O(\mu\text{-}CO_2)_6]$ unit, In^{3+} cations are normally located within the pores/channels.

In the lattice, six cages of In_{12}-GL are arranged into a ring with a diameter of ∼20 Å, and these rings pack into one-dimensional pores along the (011) axis (Figure S6). As calculated by PLATON, In_{12}-GL presents a void volume of 66.3% of the crystal volume. Though the precise solvent content cannot be determined by X-ray crystallography due to the disordered nature, the SQUEEZE routine of PLATON and thermogravimetric analysis have proven that the void spaces are filled by DMF and H_2O molecules (see the structure analysis in the Supporting Information). The thermogravimetric analysis of the as-synthesized sample (Figure S7) showed a weight loss of 6.9% before 170 °C, corresponding to the loss of 27 H_2O molecules (calculated 6.47%). With an increase in temperature from 170 to 240 °C, the second weight loss is about 24.3%, which belongs to the loss of 10 H_2O and 23 DMF molecules (calculated 24.75%).

Gas Adsorption Studies. The sample for gas adsorption studies was prepared by exchanging the reaction solvent with CH_3OH for 3 days, followed by evacuation under high vacuum at 100 °C for 10 h. The experimental maximum pore size is 18.2 Å (Figure S8), which corresponds to the pore size circled by neighboring six cages. The N_2 gas sorption measurement at 77 K (Figure 3) showed a reversible type I isotherm, characteristic of microporous materials, with a high N_2 uptake of 65 cm^3 g^{-1}. The BET surface area was estimated to be 155 m^2 g^{-1}. The CO_2 adsorption reached 16.6 and 11.0 cm^3 g^{-1}, respectively, at 273 and 298 K under 1 atm (Figure 4).

https://dx.doi.org/10.1021/acs.inorgchem.9b02763
Inorg. Chem. XXXX, XXX, XXX−XXX

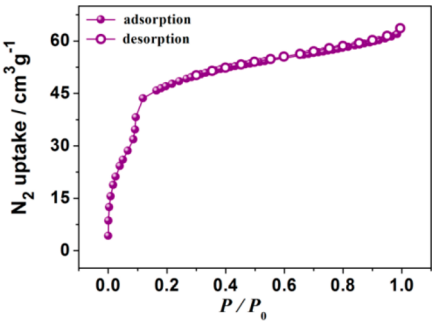

Figure 3. N_2 sorption isotherm of In_{12}-GL at 77 K.

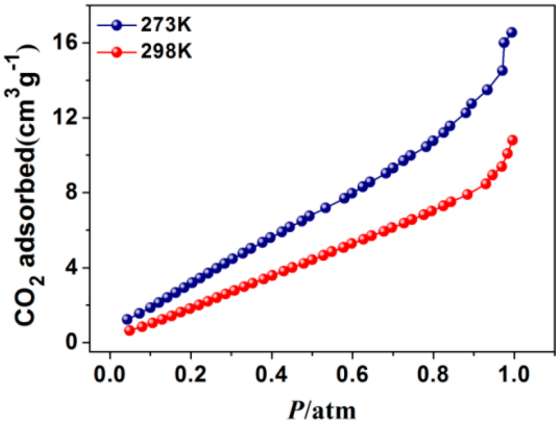

Figure 4. CO_2 sorption isotherm of In_{12}-GL at 273 and 298 K.

Table 2. Cycloaddition of CO_2 and Various Epoxides[a]

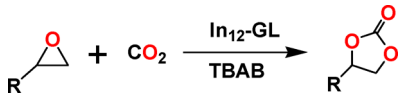

Entry	Epoxides	Product	Catalyst (mg)	T(°C)	Yield (%) [b]	TON
1			40	50	99	1295
2			40	50	95	1233
3			40	50	99	1295
4			40	50	35	454
				80	90.5	1173
5			40	50	4 [c]	
6			50 (Ligand)	60	1 [d]	
				50	9.0 [e]	
7			32.5(TBABr)	60	29 [e]	
				80	34.5 [e]	

[a]Reaction conditions unless specified otherwise: epoxide (10 mmol), catalyst (0.08 mol %), TBAB (0.1 mmol), and free solvent under 1 atm of CO_2. [b]Conversion was evaluated from GC-MS. [c]Catalyzed by In_{12}-GL alone. [d]Catalyzed by the ligand alone. [e]Catalyzed by cocatalyst TBAB alone.

Catalytic Reaction Studies. Excessive emission of the greenhouse gas CO_2 causes serious environmental problems. Conversion of CO_2 into cyclic carbonates through the cycloaddition of CO_2 with epoxides is one of the best ways for the effective elimination of CO_2 and production of valuable chemical precursors. Another famous reaction is the one-pot three-component Strecker reaction for the synthesis of α-amino nitriles, which are very useful precursors for the synthesis of α-amino acids. Though there are several reports regarding the use of MOPMs as heterogeneous catalysts for these two types of reactions,[49−53] excellent and multifunctional MOPMs are still needed to improve the catalysis under mild reaction conditions. Therefore, it is also necessary to explore catalysis of In_{12}-GL on the bases of these two reactions.

Catalytic Studies on Cycloaddition of CO_2 with Epoxides. Before the catalytic reactions, the catalyst In_{12}-GL was simply pretreated by heating at 80 °C under normal pressure for 8 h. Then solvent-free cycloaddition reactions of CO_2 with epoxides were accomplished under relatively mild conditions (1 atm and 50 °C) by adding the catalyst In_{12}-GL and cocatalyst tetrabutylammonium bromide (TBAB) for 24 h (Table 2). The yields of products were determined by GC-MS. To assess the catalytic performance of In_{12}-GL, transformation of styrene oxide with CO_2 into styrene carbonate was selected as a model reaction. In the absence of the cocatalyst TBAB, the cycloaddition reaction of CO_2 to styrene carbonate catalyzed by In_{12}-GL yielded only 4% cyclic carbonate after 24 h (Table 2, entry 5). Moreover, the effect of the ligand was not observed in catalysis of this reaction (Table 2, entry 6). Furthermore, in the absence of In_{12}-GL, the same reaction catalyzed by the cocatalyst TBAB alone gave a 9.0% yield (Table 2, entry 7). These experiments have shown that coaddition of In_{12}-GL and cocatalyst TBAB are necessary in this cycloaddition reaction. The use of the catalyst in five successive runs gave almost the same yields (Figure S9). The structural integrity of the catalyst In_{12}-GL was sustained after five cycles, as shown by PXRD and IR spectra (Figures S10 and S11). Elemental mapping spectra illustrating the C, O, and In atoms were still distributed homogeneously over the entire cage after five cycles (Figure S12). To assess the heterogeneous nature of the catalyst, In_{12}-GL was separated by hot filtration after 5 h of reaction and then the reaction that continued for 24 h showed almost no increase in product yield (Figure S13). The catalytic efficiency of In_{12}-GL was lower for a large-sized substrate such as 2-(phenoxymethyl) oxirane but improved more than double with an increase in temperature up to 80 °C (Table 2, entry 4). This size-selective catalysis may originate from the spatial confinement of the ligand and formate groups, which are encircled around the active sites of In^{3+}. The heterogeneous catalysis performance of In_{12}-GL for CO_2 fixation surpasses that of many famous MOFs such as MOF-5, Mg-MOF-74, gea-MOF-1, ZIF-8, HKUST-1, and some In-based MOFs (Table S2). Moreover, the yields for small reaction substrates are comparable to those of some of the recently reported top-performing MOF catalysts under similar conditions, such as Hf-NU-1000 (100%), MOF-892 (82%), InDCPN-Cl (93%), and PCN-700-Me_2 (93%) (Table S2).

Due to the window size of In_{12}-GL being smaller than the substrates and products (Table S3), we deduce that the catalysis should happen on the surface of In_{12}-GL. An assumptive mechanism for the catalytic fixation reaction of CO_2 by In_{12}-GL was proposed (Figure S14) similarly as other studies have described. Here, we think the In^{3+} ions may experience an intermediate state with coordination number 7

https://dx.doi.org/10.1021/acs.inorgchem.9b02763
Inorg. Chem. XXXX, XXX, XXX−XXX

in the catalytic process.[39,54] First, the oxygen atom of the epoxide ring coordinates to the In^{3+} to polarize the epoxide ring, while the CO_2 is polarized by the uncoordinated oxygen atom of μ_1-formate. Then, the polarized epoxide ring receives a nucleophilic attack by the Br^- of TBAB to form an open ring with an intermediate oxygen anion, which subsequently reacts rapidly with the polarized CO_2 molecule to generate alkyl carbonate anions. The transformation of alkyl carbonate anion into the corresponding cyclic carbonate is accomplished through a cyclization step. Therefore, it can be deduced that the overall cycloaddition process can be promoted synergistically by Lewis acidic and basic sites.

One-Pot Three-Component Strecker Reaction for Amino Nitriles. Although the one-pot synthesis of α-amino nitriles by a three-component Strecker reaction offers many advantages, the wide use of this reaction is restrained due to the low activity of some ketones. Therefore, a highly active catalyst is required to extend the types of synthesized α-amino nitriles by the use of different substituted ketones. Herein, we explored In_{12}-GL as a catalyst for this reaction. The reactions were performed in a methanol solution at room temperature, and the results are summarized in Table 3. All phenylethanones

Table 3. One-Pot Three-Component Strecker Reaction for Amino Nitriles[a]

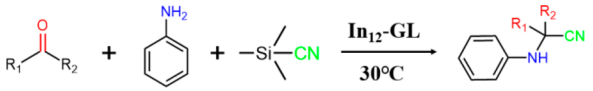

Entry	ketone	Product	t (h)	Yield (%)	TON
1	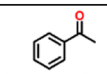	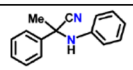	24	99	216.5
2	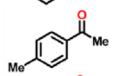	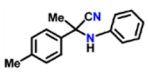	24	96	209.9
3	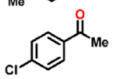	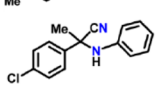	24	97	212.1
4		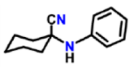	24	45	98.4
5		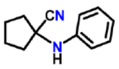	24	35	76.5
6			24	0	0
7	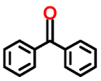	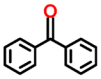	24	0	0

[a]Reaction conditions: ketone:aniline:TMSCN 1.1:1:1.1, 6 mol % of catalyst (from In_{12}-GL), N_2 atmosphere, room temperature, solvent; catalyst washed with methanol. Yield determined by GC-MS.

with electron-withdrawing or electron-donating groups gave good yields (Table 3, entries 1−3). The catalytic recyclability experiments of acetophenone and aniline for five cycles show almost the same yields (Figure S15), while the In_{12}-GL has retained almost all of its structural integrity (Figures S16−S18). The yields of conversion for cyclic ketones are lower (Table 3, entries 4 and 5), while the conversion yield is almost zero in case of bulky ketones: for example 2,4-dimethyl-3-pentanone and diphenylmethanone. The size-selective catalysis of In_{12}-GL can be still attributed to the spatial confinement of organic ligands to the active sites on the cage surface.

The effective catalytic ability of In_{12}-GL on small ketones for α-amino nitriles is comparable to that of the well-performing 3D InPF-110[45] and $[Cd_2(L)(H_2O)(DMF)]_n$[55] but is lower on the larger-sized ketones in comparison to InPF-110. The heterogeneous catalysis performances of some other indium-based MOFs have also been explored in the Strecker reaction for amino nitriles with different reaction conditions (Table S4). The catalytic pathway of In_{12}-GL for the Strecker reaction is similar to that described in the aforementioned fixation reaction of CO_2, having the synergistic catalysis of Lewis acidic and basic sites (Figure S19). Lewis acidic In^{3+} sites can catalyze ketones and intermediate aromatic aldimines. Meanwhile, the Lewis basic oxygen atom from μ_1-formate can activate TMSCN to enhance the nucleophilicity and reactivity of the cyano group for the activated intermediate aromatic aldimines.

CONCLUSION

We reported the discrete tetrahedral cage In_{12}-GL consisting of the previously unseen trimer $[In_3(OH)(\mu_2\text{-}CO_2)_3(\mu_2\text{-}HCO_2)_3]$, whose formation is directed by a semirigid tcma ligand. This cage is stable and contains a high content of active sites of In^{3+}. Just by simple pretreatment, In_{12}-GL shows effective heterogeneous catalysis on the cycloaddition of CO_2 with epoxides and the Strecker reaction for amino nitriles. The size-selective catalysis may originate from the spatial confinement around the active centers on the surface of this cage.

ASSOCIATED CONTENT

Supporting Information

The Supporting Information is available free of charge at https://pubs.acs.org/doi/10.1021/acs.inorgchem.9b02763.

Crystal structure analysis, catalytic reaction, bond distances and angles, IR, TGA, PXRD, ESI-MS, NMR data, SEM, elemental mapping spectra, and additional figures (PDF)

Accession Codes

CCDC 1953952 contains the supplementary crystallographic data for this paper. These data can be obtained free of charge via www.ccdc.cam.ac.uk/data_request/cif, or by emailing data_request@ccdc.cam.ac.uk, or by contacting The Cambridge Crystallographic Data Centre, 12 Union Road, Cambridge CB2 1EZ, UK; fax: +44 1223 336033.

AUTHOR INFORMATION

Corresponding Authors

Jian-Qiang Zeng − *School of Chemistry and Pharmaceutical Sciences, Guangxi Normal University, Guilin 541004, People's Republic of China*; Email: 178929472@qq.com

Liu-Cheng Gui − *School of Chemistry and Pharmaceutical Sciences, Guangxi Normal University, Guilin 541004, People's Republic of China*; orcid.org/0000-0002-5413-8318; Email: guiliucheng2000@163.com

Xiu-Jian Wang − *School of Chemistry and Pharmaceutical Sciences, Guangxi Normal University, Guilin 541004, People's Republic of China*; orcid.org/0000-0003-3917-6962; Email: wang1_xj@aliyun.com

Other Authors

Guang-Ming Liang − *School of Chemistry and Pharmaceutical Sciences, Guangxi Normal University, Guilin 541004, People's*

https://dx.doi.org/10.1021/acs.inorgchem.9b02763
Inorg. Chem. XXXX, XXX, XXX−XXX

Republic of China

Peng Xiong − *School of Chemistry and Pharmaceutical Sciences, Guangxi Normal University, Guilin 541004, People's Republic of China*

Khan Azam − *School of Chemistry and Pharmaceutical Sciences, Guangxi Normal University, Guilin 541004, People's Republic of China*

Qing-Ling Ni − *School of Chemistry and Pharmaceutical Sciences, Guangxi Normal University, Guilin 541004, People's Republic of China*

Complete contact information is available at:
https://pubs.acs.org/10.1021/acs.inorgchem.9b02763

Author Contributions

[§]G.-M.L. and P.X. contributed equally.

Notes

The authors declare no competing financial interest.

■ ACKNOWLEDGMENTS

This work was supported by the NSF of China (Grant No. 21861004, 21462005, 21561004), the NSF of Guangxi Province, China (No. 2016GXNSFDA380004 and 2018GXNSFAA138135), and the innovation project of Guangxi Graduate Education (YCBZ2016003). We thank the staff of the BL17B beamline at the National Facility for Protein Sciences Shanghai (NFPS) at SSRF.

■ REFERENCES

(1) Furukawa, H.; Cordova, K. E.; O'Keeffe, M.; Yaghi, O. M. The Chemistry and Applications of Metal-Organic Frameworks. *Science* **2013**, *341*, 1230444.

(2) Lee, J. Y.; Farha, O. K.; Roberts, J.; Scheidt, K. A.; Nguyen, S. B. T.; Hupp, J. T. Metal-Organic Framework Materials as Catalysts. *Chem. Soc. Rev.* **2009**, *38*, 1450−1459.

(3) Yang, Q.; Xu, Q.; Jiang, H.-L. Metal-Organic Frameworks Meet Metal Nanoparticles: Synergistic Effect for Enhanced Catalysis. *Chem. Soc. Rev.* **2017**, *46*, 4774−4808.

(4) Liu, J.; Chen, L.; Cui, H.; Zhang, J.; Zhang, L.; Su, C.-Y. Applications of Metal-Organic Frameworks in Heterogeneous Supramolecular Catalysis. *Chem. Soc. Rev.* **2014**, *43*, 6011−6061.

(5) Li, B.; Ju, Z.; Zhou, M.; Su, K.; Yuan, D. A Reusable MOF-Supported Single-Site Zinc (II) Catalyst for Efficient Intramolecular Hydroamination of o-Alkynylanilines. *Angew. Chem., Int. Ed.* **2019**, *58*, 7687−7691.

(6) Liu, J.; Fan, Y.-Z.; Li, X.; Wei, Z.; Xu, Y.-W.; Zhang, L.; Su, C.-Y. A Porous Rhodium (III)-porphyrin Metal-Organic Framework as an Efficient and Selective Photocatalyst for CO_2 Reduction. *Appl. Catal., B* **2018**, *231*, 173−181.

(7) Wang, Y.; Cui, H.; Wei, Z.; Wang, H.-P.; Zhang, L.; Su, C.-Y. Engineering Catalytic Coordination Space in a Chemically Stable Ir-porphyrin MOF with a Confinement Effect Inverting Conventional Si-H Insertion Chemoselectivity. *Chem. Sci.* **2017**, *8* (1), 775−780.

(8) Corma, A.; Garcia, H.; Llabres i Xamena, F. X. Engineering Metal Organic Frameworks for Heterogeneous Catalysis. *Chem. Rev.* **2010**, *110*, 4606−4655.

(9) Johnson, J. A.; Zhang, X.; Reeson, T. C.; Chen, Y.-S.; Zhang, J. Facile Control of the Charge Density and Photocatalytic Activity of an Anionic Indium Porphyrin Framework via in Situ Metalation. *J. Am. Chem. Soc.* **2014**, *136*, 15881−15884.

(10) Elcheikh Mahmoud, M.; Audi, H.; Assoud, A.; Ghaddar, T. H.; Hmadeh, M. Metal-Organic Framework Photocatalyst Incorporating Bis(4'-(4-carboxyphenyl)-terpyridine) Ruthenium (II) for Visible-Light-Driven Carbon Dioxide Reduction. *J. Am. Chem. Soc.* **2019**, *141*, 7115−7121.

(11) Hwang, Y. K.; Hong, D.-Y.; Chang, J.-S.; Jhung, S. H.; Seo, Y.-K.; Kim, J.; Vimont, A.; Daturi, M.; Serre, C.; Ferey, G. Amine Grafting on Coordinatively Unsaturated Metal Centers of MOFs: Consequences for Catalysis and Metal Encapsulation. *Angew. Chem., Int. Ed.* **2008**, *47* (22), 4144−4148.

(12) Ji, S.; Chen, Y.; Zhao, S.; Chen, W.; Shi, L.; Wang, Y.; Dong, J.; Li, Z.; Li, F.; Chen, C.; Peng, Q.; Li, J.; Wang, D.; Li, Y. Atomically Dispersed Ruthenium Species Inside Metal-Organic Frameworks: Combining the High Activity of Atomic Sites and the Molecular Sieving Effect of MOFs. *Angew. Chem., Int. Ed.* **2019**, *58*, 4271−4275.

(13) Carné-Sánchez, A.; Albalad, J.; Grancha, T.; Imaz, I.; Juanhuix, J.; Larpent, P.; Furukawa, S.; Maspoch, D. Postsynthetic Covalent and Coordination Functionalization of Rhodium(II)-Based Metal-Organic Polyhedra. *J. Am. Chem. Soc.* **2019**, *141*, 4094−4102.

(14) Lorzing, G. R.; Gosselin, E. J.; Trump, B. A.; York, A. H. P.; Sturluson, A.; Rowland, C. A.; Yap, G. P. A.; Brown, C. M.; Simon, C. M.; Bloch, E. D. Understanding Gas Storage in Cuboctahedral Porous Coordination Cages. *J. Am. Chem. Soc.* **2019**, *141*, 12128−12138.

(15) Lorzing, G. R.; Gosselin, E. J.; Lindner, B. S.; Bhattacharjee, R.; Yap, G. P. A.; Caratzoulas, S.; Bloch, E. D. Design and Synthesis of Capped-Paddle Wheel Based Porous Coordination Cages. *Chem. Commun.* **2019**, *55*, 9527−9530.

(16) Luo, Y.-C.; Chu, K.-L.; Shi, J.-Y.; Wu, D.-J.; Wang, X.-D.; Mayor, M.; Su, C.-Y. Heterogenization of Photochemical Molecular Devices: Embedding a Metal−Organic Cage into a ZIF-8-Derived Matrix to Promote Proton and Electron Transfer. *J. Am. Chem. Soc.* **2019**, *141*, 13057−13065.

(17) Zhou, X.-P.; Wu, Y.; Li, D. Polyhedral Metal-Imidazolate Cages: Control of Self-Assembly and Cage to Cage Transformation. *J. Am. Chem. Soc.* **2013**, *135*, 16062−16065.

(18) Jiao, J.; Tan, C.; Li, Z.; Liu, Y.; Han, X.; Cui, Y. Design and Assembly of Chiral Coordination Cages for Asymmetric Sequential Reactions. *J. Am. Chem. Soc.* **2018**, *140*, 2251−2259.

(19) Pullen, S.; Clever, G. H. Mixed-Ligand Metal−Organic Frameworks and Heteroleptic Coordination Cages as Multifunctional Scaffolds − A Comparison. *Acc. Chem. Res.* **2018**, *51*, 3052−3064.

(20) Li, K.; Zhang, L.-Y.; Yan, C.; Wei, S.-C.; Pan, M.; Zhang, L.; Su, C.-Y. Stepwise Assembly of Pd6(RuL3)8 Nanoscale Rhombododecahedral Metal−Organic Cages via Metalloligand Strategy for Guest Trapping and Protection. *J. Am. Chem. Soc.* **2014**, *136*, 4456−4459.

(21) Zeng, L.; Xiao, Y.; Jiang, J.; Fang, H.; Ke, Z.; Chen, L.; Zhang, J. Hierarchical Gelation of a Pd12L24 Metal−Organic Cage Regulated by Cholesteryl Groups. *Inorg. Chem.* **2019**, *58*, 10019−10027.

(22) Beyzavi, M. H.; Klet, R. C.; Tussupbayev, S.; Borycz, J.; Vermeulen, N. A.; Cramer, C. J.; Stoddart, J. F.; Hupp, J. T.; Farha, O. K. A Hafnium-Based Metal-Organic Framework as an Efficient and Multifunctional Catalyst for Facile CO_2 Fixation and Regioselective and Enantioretentive Epoxide Activation. *J. Am. Chem. Soc.* **2014**, *136*, 15861−15864.

(23) Yoon, M.; Srirambalaji, R.; Kim, K. Homochiral Metal-Organic Frameworks for Asymmetric Heterogeneous Catalysis. *Chem. Rev.* **2012**, *112*, 1196−1231.

(24) Liu, Y.; Xuan, W.; Cui, Y. Engineering Homochiral Metal-Organic Frameworks for Heterogeneous Asymmetric Catalysis and Enantioselective Separation. *Adv. Mater.* **2010**, *22*, 4112−4135.

(25) Huang, Y.; Liu, T.; Lin, J.; Lü, J.; Lin, Z.; Cao, R. Homochiral Nickel Coordination Polymers Based on Salen(Ni) Metalloligands: Synthesis, Structure, and Catalytic Alkene Epoxidation. *Inorg. Chem.* **2011**, *50*, 2191−2198.

(26) Ju, Z.; Yan, S.; Yuan, D. De Novo Tailoring Pore Morphologies and Sizes for Different Substrates in a Urea-Containing MOFs Catalytic Platform. *Chem. Mater.* **2016**, *28*, 2000−2010.

(27) Carrington, E. J.; McAnally, C. A.; Fletcher, A. J.; Thompson, S. P.; Warren, M.; Brammer, L. Solvent-switchable Continuous-breathing Behaviour in a Diamondoid Metal-Organic Framework and its Influence on CO_2 Versus CH_4 Selectivity. *Nat. Chem.* **2017**, *9*, 882−889.

(28) Zhou, T.; Du, Y.; Borgna, A.; Hong, J.; Wang, Y.; Han, J.; Zhang, W.; Xu, R. Post-synthesis modification of a Metal-Organic

Framework to Construct a Bifunctional Photocatalyst for Hydrogen Production. *Energy Environ. Sci.* **2013**, *6*, 3229−3234.
(29) He, H.; Sun, Q.; Gao, W.; Perman, J. A.; Sun, F.; Zhu, G.; Aguila, B.; Forrest, K.; Space, B.; Ma, S. A Stable Metal-Organic Framework Featuring a Local Buffer Environment for Carbon Dioxide Fixation. *Angew. Chem., Int. Ed.* **2018**, *57*, 4657−4662.
(30) Li, X.; Guo, Z.; Xiao, C.; Goh, T. W.; Tesfagaber, D.; Huang, W. Tandem Catalysis by Palladium Nanoclusters Encapsulated in Metal-Organic Frameworks. *ACS Catal.* **2014**, *4*, 3490−3497.
(31) Masoomi, M. Y.; Morsali, A.; Dhakshinamoorthy, A.; Garcia, H. Mixed-Metal MOFs: Unique Opportunities in Metal-Organic Framework (MOF) Functionality and Design. *Angew. Chem., Int. Ed.* **2019**, *58*, 15188−15205.
(32) Perry IV, J. J.; Perman, J. A.; Zaworotko, M. J. Design and Synthesis of Metal-Organic Frameworks Using Metal-Organic Polyhedra as Supermolecular Building Blocks. *Chem. Soc. Rev.* **2009**, *38*, 1400−1417.
(33) Zheng, S.-T.; Zhao, X.; Lau, S.; Fuhr, A.; Feng, P.; Bu, X. Entrapment of Metal Clusters in Metal-Organic Framework Channels by Extended Hooks Anchored at Open Metal Sites. *J. Am. Chem. Soc.* **2013**, *135*, 10270−10273.
(34) Jiao, L.; Wang, Y.; Jiang, H.-L.; Xu, Q. Metal-Organic Frameworks as Platforms for Catalytic Applications. *Adv. Mater.* **2018**, *30*, 1703663.
(35) Dhakshinamoorthy, A.; Li, Z.; Garcia, H. Catalysis and Photocatalysis by Metal Organic Frameworks. *Chem. Soc. Rev.* **2018**, *47*, 8134−8172.
(36) Liang, L.; Liu, C.; Jiang, F.; Chen, Q.; Zhang, L.; Xue, H.; Jiang, H.-L.; Qian, J.; Yuan, D.; Hong, M. In Situ Click Chemistry Generation of Cyclooxygenase-2 Inhibitors. *Nat. Commun.* **2017**, *8* (1), 1−10.
(37) Seo, J. S.; Whang, D.; Lee, H.; Jun, S. I.; Oh, J.; Jeon, Y. J.; Kim, K. A Homochiral Metal-Organic Porous Material for Enantioselective Separation and Catalysis. *Nature* **2000**, *404*, 982−986.
(38) Zheng, B.; Sun, X.; Li, G.; Cairns, A. J.; Kravtsov, V. C.; Huo, Q.; Liu, Y.; Eddaoudi, M. Solvent-Controlled Assembly of Ionic Metal-Organic Frameworks Based on Indium and Tetracarboxylate Ligand: Topology Variety and Gas Sorption Properties. *Cryst. Growth Des.* **2016**, *16*, 5554−5562.
(39) Yuan, Y.; Li, J.; Sun, X.; Li, G.; Liu, Y.; Verma, G.; Ma, S. Indium-Organic Frameworks Based on Dual Secondary Building Units Featuring Halogen-Decorated Channels for Highly Effective CO_2 Fixation. *Chem. Mater.* **2019**, *31*, 1084−1091.
(40) Du, X.; Fan, R.; Qiang, L.; Song, Y.; Xing, K.; Chen, W.; Wang, P.; Yang, Y. Unusually Flexible Indium (III) Metal-Organic Polyhedra Materials for Detecting Trace Amounts of Water in Organic Solvents and High Proton Conductivity. *Inorg. Chem.* **2017**, *56*, 3429−3439.
(41) Leng, F.; Liu, H.; Ding, M.; Lin, Q.; Jiang, H.-L. Boosting Photocatalytic Hydrogen Production of Porphyrinic MOFs: The Metal Location in Metalloporphyrin Matters. *ACS Catal.* **2018**, *8*, 4583−4590.
(42) Du, M.; Chen, M.; Yang, X.-G.; Wen, J.; Wang, X.; Fang, S.-M.; Liu, C.-S. A Channel-type Mesoporous In(III)-carboxylate Coordination Framework with High Physicochemical Stability for Use as an Electrode Material in Supercapacitors. *J. Mater. Chem. A* **2014**, *2*, 9828−9834.
(43) Li, Q.; Xue, D.-X.; Zhang, Y.-F.; Zhang, Z.-H.; Gao, Z.; Bai, J. A Dual-functional Indium-Organic Framework Towards Organic Pollutant Decontamination via Physically Selective Adsorption and Chemical Photodegradation. *J. Mater. Chem. A* **2017**, *5*, 14182−14189.
(44) Zhou, M.; Ju, Z.; Yuan, D. A new Metal-Organic Framework Constructed from Cationic Nodes and Cationic Linkers for Highly Efficient Anion Exchange. *Chem. Commun.* **2018**, *54*, 2998−3001.
(45) Reinares-Fisac, D.; Aguirre-Díaz, L. M.; Iglesias, M.; Natalia Snejko, N.; Gutiérrez-Puebla, E.; Monge, M. A.; Gándara, F. A Mesoporous Indium Metal-Organic Framework: Remarkable Advances in Catalytic Activity for Strecker Reaction of Ketones. *J. Am. Chem. Soc.* **2016**, *138*, 9089−9092.
(46) Liu, Y.; Eubank, J. F.; Cairns, A. J.; Eckert, J.; Kravtsov, V. Ch.; Luebke, R.; Eddaoudi, M. Assembly of Metal-Organic Frameworks (MOFs) Based on Indium-Trimer Building Blocks: A Porous MOF with soc Topology and High Hydrogen Storage. *Angew. Chem., Int. Ed.* **2007**, *46*, 3278−3283.
(47) Zhang, J.-W.; Ji, W.-J.; Hu, M.-C.; Li, S.-N.; Jiang, Y.-C.; Zhang, X.-M.; Qu, P.; Zhai, Q.-G. A superstable 3p-block metal−organic framework platform towards prominent CO_2 and C1/C2- hydrocarbon uptake and separation performance and strong Lewis acid catalysis for CO_2 fixation. *Inorg. Chem. Front.* **2019**, *6*, 813−819.
(48) Huang, P.; Chen, C.; Wu, M.; Jiang, F.; Hong, M. An indium−organic framework for the efficient storage of light hydrocarbons and selective removal of organic dyes. *Dalton Trans.* **2019**, *48*, 5527−5533.
(49) Verma, A.; De, D.; Tomar, K.; Bharadwaj, P. K. An Amine Functionalized Metal-Organic Framework as an Effective Catalyst for Conversion of CO_2 and Biginelli Reactions. *Inorg. Chem.* **2017**, *56*, 9765−9771.
(50) Xu, W.; Chen, H.; Jie, K.; Yang, Z.; Li, T.; Dai, S. Entropy-Driven Mechanochemical Synthesis of Polymetallic Zeolitic Imidazolate Frameworks for CO_2 Fixation. *Angew. Chem., Int. Ed.* **2019**, *58*, 5018−5022.
(51) Zhang, G.; Yang, H.; Fei, H. Unusual Missing Linkers in an Organosulfonate-Based Primitive-Cubic (pcu)-Type Metal-Organic Framework for CO_2 Capture and Conversion under Ambient Conditions. *ACS Catal.* **2018**, *8*, 2519−2525.
(52) Liu, J.; Fan, Y.-Z.; Li, X.; Xu, Y.-W.; Zhang, L.; Su, C.-Y. Catalytic Space Engineering of Porphyrin Metal-Organic Frameworks for Combined CO_2 Capture and Conversion at a Low Concentration. *ChemSusChem* **2018**, *11* (14), 2340−2347.
(53) Wang, X.; Gao, W.-Y.; Niu, Z.; Wojtas, L.; Perman, J. A.; Chen, Y.-S.; Li, Z.; Aguila, B.; Ma, S. A Metal-Metalloporphyrin Framework Based on an Octatopic Porphyrin Ligand for Chemical Fixation of CO_2 with Aziridines. *Chem. Commun.* **2018**, *54*, 1170−1173.
(54) Aguirre-Diaz, L. M.; Gandara, F.; Iglesias, M.; Snejko, N.; Gutierrez-Puebla, E.; Monge, M. A. Tunable Catalytic Activity of Solid Solution Metal-Organic Frameworks in One-Pot Multicomponent Reactions. *J. Am. Chem. Soc.* **2015**, *137* (19), 6132−6135.
(55) Verma, A.; Tomar, K.; Bharadwaj, P. K. Chiral Cadmium(II) Metal−Organic Framework From an Achiral Ligand by Spontaneous Resolution: an Efficient Heterogeneous Catalyst for the Strecker Reaction of Ketones. *Inorg. Chem.* **2017**, *56*, 13629−13633.

https://dx.doi.org/10.1021/acs.inorgchem.9b02763
Inorg. Chem. XXXX, XXX, XXX−XXX